

---

# CMS Physics Analysis Summary

---

Contact: cms-pag-conveners-higgs@cern.ch

2012/11/13

## Search for MSSM Neutral Higgs Bosons Decaying to Tau Pairs in pp Collisions

The CMS Collaboration

### Abstract

A search for neutral Higgs bosons in the minimal supersymmetric extension of the standard model (MSSM) decaying to tau pairs is performed using events recorded by the CMS experiment at the LHC in 2011 and 2012 at a center-of-mass energy of 7 TeV and 8 TeV respectively. The dataset corresponds to an integrated luminosity of  $17 \text{ fb}^{-1}$ , with  $4.9 \text{ fb}^{-1}$  at 7 TeV and  $12.1 \text{ fb}^{-1}$  at 8 TeV. To enhance the sensitivity to neutral MSSM Higgs bosons, the search includes the case where the Higgs boson is produced in association with a b-quark jet. No excess is observed in the tau-pair invariant-mass spectrum. Exclusion limits in the MSSM parameter space of  $M_A$  and  $\tan\beta$  in the  $m_h^{\max}$  scenario are presented.



## 1 Introduction

Experimental evidence from a large number of high energy experiments has shown an overwhelming success of the Standard Model (SM) of fundamental interactions, although some questions remain unanswered like the origin of mass of elementary particles. In the SM [1–3], this is achieved via the Higgs mechanism [4–9], which also predicts the existence of a scalar Higgs boson. However, the SM Higgs boson suffers from quadratically divergent self-energy corrections at high energy. Numerous extensions to the SM have been proposed to address these divergencies. In the model of supersymmetry (SUSY) [10, 11], a symmetry between fundamental bosons and fermions, a cancellation of these divergencies occurs. The Higgs sector of the minimal supersymmetric standard model (MSSM) [12, 13] has two scalar doublets which results in five physical Higgs bosons: a light and heavy CP-even  $h$  and  $H$ , the CP-odd  $A$  and the charged Higgs boson  $H^\pm$ . At lowest order the Higgs sector can be expressed in terms of two parameters which are usually chosen as  $\tan\beta$ , the ratio of the two vacuum expectation values, and the mass of the CP-odd boson,  $M_A$ .

The dominant neutral MSSM Higgs boson production mechanism is the gluon-fusion process,  $gg \rightarrow h, H, A$ , for small and moderate values of  $\tan\beta$ . At large values of  $\tan\beta$  the b-associated production is the dominant contribution, due to the enhanced bottom Yukawa coupling. In the region of large  $\tan\beta$  the branching ratio to tau leptons is enhanced, making the search for neutral MSSM Higgs bosons in the di- $\tau$  final state of particular interest.

This Summary reports a search for neutral MSSM Higgs bosons in  $pp$  collisions at  $\sqrt{s} = 7$  TeV and 8 TeV at the LHC. The data were recorded by the Compact Muon Solenoid experiment (CMS) [14] in 2011 and 2012 and correspond to an integrated luminosity of  $17 \text{ fb}^{-1}$ , with  $4.9 \text{ fb}^{-1}$  at 7 TeV and  $12.1 \text{ fb}^{-1}$  at 8 TeV. Four different  $\tau\tau$  final states are studied where one or two taus decay leptonically  $e\tau_h, \mu\tau_h, e\mu$  and  $\mu\mu$ , where  $\tau_h$  denotes a hadronic decay of a  $\tau$ . These results are an extension of a previous search by the CMS experiment [15] and are similar to those performed by the the ATLAS experiment [16], the Tevatron [17–19], and is complimentary to the MSSM Higgs search at LEP [20].

Traditionally, searches for MSSM Higgs bosons are expressed in terms of benchmark scenarios where the lowest-order parameters  $\tan\beta$  and  $M_A$  are varied, while fixing the other parameters that enter through radiative corrections to certain benchmark values. In this study, the  $m_h^{\max}$  scenario [21, 22] is used as it yields conservative expected limits in the  $\tan\beta$  and  $M_A$  plane.

Recently the CMS and ATLAS experiments have reported the observation of a new boson with mass in the range 125–126 GeV [23, 24]. If this new boson is interpreted as the light scalar MSSM Higgs  $h$ , part of the  $\tan\beta$  and  $M_A$  parameter space in the  $m_h^{\max}$  scenario is excluded. However, changes in the stop mixing parameter open up a large region of the allowed parameter space [25].

## 2 Trigger and Event Selection

The trigger selection requires a combination of electron, muon and tau trigger objects [26–28]. The identification criteria and transverse momentum thresholds of these objects were progressively tightened as the LHC instantaneous luminosity increased over the data-taking period.

A particle-flow algorithm [29–31] is used to combine information from all CMS subdetectors to identify and reconstruct individual particles in the event, namely muons, electrons, photons, and charged and neutral hadrons. From the resulting particle list jets, hadronically decaying taus, and missing transverse energy ( $\cancel{E}_T$ ), defined as the magnitude of the vector sum of the

transverse momenta, are reconstructed using the anti- $k_T$  jet algorithm [32, 33] with a distance parameter of  $R = 0.5$ . Hadronically-decaying taus are reconstructed using the hadron plus strips (HPS) algorithm, which considers candidates with one charged pion and up to two neutral pions or three charged pions [34]. To tag jets coming from b-quark decays the Combined Secondary Vertex (CSV) algorithm is used. This algorithm is based on the reconstruction of secondary vertices, together with track-based lifetime information [35].

In the  $e\tau_h$  and  $\mu\tau_h$  final states, events are selected in the 2011 (2012) dataset with an electron of  $p_T > 20$  GeV (24 GeV) or a muon of  $p_T > 17$  GeV (20 GeV) and  $|\eta| < 2.1$  and an oppositely charged  $\tau_h$  of  $p_T > 20$  GeV and  $|\eta| < 2.3$ . To reduce the contamination of  $Z \rightarrow ee, \mu\mu$  background, events with more than one electron or muon of  $p_T > 15$  GeV are rejected and in addition,  $\cancel{E}_T$  is required to be larger than 25 GeV in the  $e\tau_h$  final state. In the  $e\mu$  and  $\mu\mu$  final states events with two oppositely charged leptons are selected, where the highest- $p_T$  lepton is required to have  $p_T > 20$  GeV and the second-highest- $p_T$  lepton  $p_T > 10$  GeV. Muons with  $|\eta| < 2.1$  and electrons with  $|\eta| < 2.3$  are used.

An average of 10 (20) proton-proton interactions occurred per LHC bunch crossing in 2011 (2012), making the reconstruction of physics objects challenging. For each reconstructed collision vertex the sum of the  $p_T^2$  of all tracks associated to the vertex is computed and the one with the largest value is taken as the primary collision vertex. In order to mitigate the effects on the reconstruction of  $\cancel{E}_T$ , a multivariate regression correction is used where the inputs are separated in those components coming from the primary vertex and those which are not. The overall correction improves the  $\cancel{E}_T$  resolution in  $Z \rightarrow \mu\mu$  events by roughly a factor of two when 25 additional pile-up events are present.

Electrons and muons from  $\tau$  decays are expected to be isolated in the detector, while leptons from heavy-flavour (c and b) decays and decays in flight are expected to be found inside jets. A measure of isolation is used to discriminate the signal from the QCD multijet background, based on the charged hadrons, photons, and neutral hadrons falling within a cone around the lepton momentum direction. A correction is applied to the isolation to reduce the effects of pile-up. For charged particles, only those associated with the primary vertex are considered and for neutral particles, a correction is applied by subtracting the energy deposited in the isolation cone by charged particles not associated with the primary vertex, multiplied by a factor of 0.5 which approximately corresponds to the ratio of neutral to charged hadron production in the hadronization process of pile-up interactions. An  $\eta$ ,  $p_T$ , and lepton-flavor dependent threshold on the isolation variable of less than roughly 10% of the candidate  $p_T$  is applied.

To correct for the contribution to the jet energy due to pile-up, a median energy density ( $\rho$ ) is determined event by event. The pile-up contribution to the jet energy is estimated as the product of  $\rho$  and the area of the jet and subsequently subtracted from the jet transverse energy [36]. In the fiducial region for jets of  $|\eta| < 4.7$ , jet energy corrections are also applied as a function of the jet  $E_T$  and  $\eta$  [37].

For taus decaying hadronically, the isolation variable is calculated using a multivariate *Boosted Decision Tree (BDT)* technique based on the neighboring reconstructed particles. Rings of radius  $\Delta R = \sqrt{\Delta\phi^2 + \Delta\eta^2}$  are formed in the vicinity of the identified  $\tau_h$  candidate and the moments of the energy deposits in  $\eta$  and  $\phi$  and the energy density  $\rho$  in the event is used to define the isolation variables.

In order to reject events coming from W+jets background a dedicated selection is applied. In the  $e\tau_h$  and  $\mu\tau_h$  final states, the transverse mass of the electron or muon and the  $\cancel{E}_T$ ,  $M_T =$

$\sqrt{2p_T E_T(1 - \cos \Delta\phi)}$ , is required to be less than 40 GeV, where  $p_T$  is the lepton transverse momentum and  $\Delta\phi$  is the difference in  $\phi$  of the lepton and  $E_T$  vector. In the  $e\mu$  and the  $\mu\mu$  final states, a discriminator is formed by considering the bisector of the directions of the visible tau decay products transverse to the beam direction, denoted as the  $\zeta$  axis. From the projections of the visible decay product momenta and the  $E_T$  vector onto the  $\zeta$  axis, two values are calculated:  $P_\zeta = p_{T,1} \cdot \zeta + p_{T,2} \cdot \zeta + E_T \cdot \zeta$  ;  $P_\zeta^{\text{vis}} = p_{T,1} \cdot \zeta + p_{T,2} \cdot \zeta$  , where  $p_{T,1}$  and  $p_{T,2}$  indicate the transverse momentum of two reconstructed leptons.  $e\mu$  and the  $\mu\mu$  events are selected with  $P_\zeta - 0.85 \cdot P_\zeta^{\text{vis}} > -25$  GeV.

To further enhance the sensitivity of the search for Higgs bosons, the sample of selected events is split into two mutually exclusive categories:

- **B-Tag:** This event category is intended to exploit the production of Higgs bosons in association with  $b$ -quarks which is enhanced in the MSSM. At least one  $b$ -tagged jet with  $p_T > 20$  GeV is required and not more than one jet with  $p_T > 30$  GeV.
- **No B-Tag:** This event category is mainly sensitive to the gluon-fusion Higgs production mechanism. Events are required to have no  $b$ -tagged jets with  $p_T > 20$  GeV.

The observed number of events for each category, as well as the expected number of events from various background processes, are shown in Tables 1–4 together with expected signal yields and efficiencies.

The largest source of background events comes from  $Z \rightarrow \tau\tau$ , which is estimated using a sample of  $Z \rightarrow \mu\mu$  events where the reconstructed muons are replaced by the reconstructed particles from simulated tau decays. The normalization for this process is determined from the measurement of the  $Z \rightarrow \mu\mu$  yield in data. Another significant source of background is QCD multijet events where one jet is misidentified as an isolated electron or muon, and a second jet as  $\tau_h$ . Events from  $W+jets$  in which there is a jet misidentified as a  $\tau_h$  are also a source of background. The rates for these processes are estimated using the number of observed same-charge tau pair events, and from events with large transverse mass, respectively. Other background processes include  $t\bar{t}$  production and  $Z \rightarrow ee/\mu\mu$  events, particularly in the  $e\tau_h$  channel due to the 2–3% probability for electrons to be misidentified as  $\tau_h$  [34]. In the  $e\mu$  final state, the  $W+jets$  and multijet background events are obtained by measuring the number of events with one good lepton and a second one which passes relaxed selection criteria, but fails the nominal lepton selection. This sample is extrapolated to the signal region using the efficiencies for such loose lepton candidates to pass the nominal lepton selection. These efficiencies are measured in data using observed multijet events. The shape of the  $t\bar{t}$  and di-boson backgrounds are estimated from simulation using MADGRAPH [38] and PYTHIA [39], respectively. The event yields are determined from measurements in background-enriched regions.

To model the MSSM Higgs boson signals the event generators PYTHIA and POWHEG [40] are used and the TAUOLA [41] package is used for tau decays in all cases. In all Monte Carlo samples, additional interations are simulated and reweighted to the observed pile-up distribution. The missing transverse energy response from simulation is corrected using a prescription [42] where  $Z$  bosons are reconstructed in the dimuon channel, where the correction is applied as a function of the  $Z$  boson transverse momentum.

### 3 Tau-pair invariant mass reconstruction

To distinguish the signal of Higgs bosons from the background, the tau-pair mass is reconstructed using a maximum likelihood technique [15]. The algorithm computes the tau-pair mass that is most compatible with the observed momenta of visible tau decay products and

Table 1: Number of expected events in the two event categories in the  $\mu\tau_h$  channel, where the combined statistical and systematic uncertainty is shown. The expected signal yields and efficiencies for a MSSM Higgs boson with  $M_A = 160$  GeV are also given.

| Process                         | <i>B</i> -Tag  | No <i>B</i> -Tag  |
|---------------------------------|----------------|-------------------|
| $Z \rightarrow \tau\tau$        | $928 \pm 65$   | $78323 \pm 5026$  |
| QCD                             | $531 \pm 84$   | $15733 \pm 1172$  |
| W+jets                          | $181 \pm 42$   | $9065 \pm 711$    |
| $Z+jets$ (1/jet faking $\tau$ ) | $17 \pm 5$     | $1459 \pm 428$    |
| $t\bar{t}$                      | $122 \pm 23$   | $368 \pm 45$      |
| Dibosons                        | $37 \pm 6$     | $319 \pm 48$      |
| Total Background                | $1816 \pm 117$ | $105267 \pm 5216$ |
| $H \rightarrow \tau\tau$        | $50 \pm 4$     | $585 \pm 33$      |
| Data                            | 1726           | 102728            |

Signal Efficiency

|                       |                      |                      |
|-----------------------|----------------------|----------------------|
| $gg \rightarrow \Phi$ | $1.99 \cdot 10^{-4}$ | $1.78 \cdot 10^{-2}$ |
| $bb \rightarrow \Phi$ | $2.74 \cdot 10^{-3}$ | $1.62 \cdot 10^{-2}$ |

Table 2: Number of expected events in the two event categories in the  $e\tau_h$  channel, where the combined statistical and systematic uncertainty is shown. The expected signal yields and efficiencies for a MSSM Higgs boson with  $M_A = 160$  GeV are also given.

| Process                         | <i>B</i> -Tag | No <i>B</i> -Tag |
|---------------------------------|---------------|------------------|
| $Z \rightarrow \tau\tau$        | $333 \pm 24$  | $24235 \pm 1533$ |
| QCD                             | $178 \pm 27$  | $8359 \pm 619$   |
| W+jets                          | $95 \pm 24$   | $3978 \pm 316$   |
| $Z+jets$ (1/jet faking $\tau$ ) | $74 \pm 14$   | $5518 \pm 298$   |
| $t\bar{t}$                      | $45 \pm 8$    | $166 \pm 20$     |
| Dibosons                        | $17 \pm 3$    | $131 \pm 20$     |
| Total Background                | $742 \pm 45$  | $42387 \pm 1876$ |
| $H \rightarrow \tau\tau$        | $23 \pm 2$    | $264 \pm 14$     |
| Data                            | 695           | 42124            |

Signal Efficiency

|                       |                      |                      |
|-----------------------|----------------------|----------------------|
| $gg \rightarrow \Phi$ | $8.16 \cdot 10^{-5}$ | $7.94 \cdot 10^{-3}$ |
| $bb \rightarrow \Phi$ | $1.27 \cdot 10^{-3}$ | $7.25 \cdot 10^{-3}$ |

the missing transverse energy reconstructed in the event. Free parameters, corresponding to the missing neutrino momenta, are subject to kinematic constraints and are eliminated by marginalization. The algorithm yields a tau-pair mass distribution consistent with the true value and a width of 15-20%.

## 4 Systematic uncertainties

Various imperfectly known or simulated effects can alter the shape and normalization of the invariant mass spectrum. The main contributions to the normalization uncertainty include the uncertainty in the total integrated luminosity (4.5%) [43], jet energy scale (2–5% depending on  $\eta$

Table 3: Number of expected events in the two event categories in the  $e\mu$  channel, where the combined statistical and systematic uncertainty is shown. The expected signal yields and efficiencies for a MSSM Higgs boson with  $M_A = 160$  GeV are also given.

| Process                  | <i>B</i> -Tag  | <i>No B</i> -Tag |
|--------------------------|----------------|------------------|
| $Z \rightarrow \tau\tau$ | $572 \pm 21$   | $43382 \pm 1355$ |
| QCD                      | $144 \pm 41$   | $3127 \pm 773$   |
| $t\bar{t}$               | $1203 \pm 139$ | $2069 \pm 194$   |
| Dibosons                 | $263 \pm 40$   | $2183 \pm 286$   |
| Total Background         | $2182 \pm 152$ | $50761 \pm 1598$ |
| $H \rightarrow \tau\tau$ | $27 \pm 2$     | $305 \pm 12$     |
| Data                     | 2024           | 51524            |

Signal Efficiency

|                       |                      |                      |
|-----------------------|----------------------|----------------------|
| $gg \rightarrow \Phi$ | $1.06 \cdot 10^{-4}$ | $9.52 \cdot 10^{-3}$ |
| $bb \rightarrow \Phi$ | $1.50 \cdot 10^{-3}$ | $8.30 \cdot 10^{-3}$ |

Table 4: Number of expected events in the two event categories in the  $\mu\mu$  channel, where the combined statistical and systematic uncertainty is shown. The expected signal yields and efficiencies for a MSSM Higgs boson with  $M_A = 160$  GeV are also given.

| Process                  | <i>B</i> -Tag  | <i>No B</i> -Tag     |
|--------------------------|----------------|----------------------|
| $Z \rightarrow \tau\tau$ | $155 \pm 8$    | $19248 \pm 897$      |
| QCD                      | $34 \pm 30$    | $1546 \pm 117$       |
| W+jets                   | $3 \pm 3$      | $122 \pm 23$         |
| $Z \rightarrow \mu\mu$   | $5783 \pm 935$ | $1956286 \pm 131990$ |
| $t\bar{t}$               | $246 \pm 33$   | $5938 \pm 555$       |
| Dibosons                 | $37 \pm 10$    | $7066 \pm 1726$      |
| Total Background         | $6258 \pm 936$ | $1990206 \pm 132006$ |
| $H \rightarrow \tau\tau$ | $10 \pm 6$     | $163 \pm 10$         |
| Data                     | 6175           | 1953340              |

Signal Efficiency

|                       |                      |                      |
|-----------------------|----------------------|----------------------|
| $gg \rightarrow \Phi$ | $3.05 \cdot 10^{-5}$ | $5.12 \cdot 10^{-3}$ |
| $bb \rightarrow \Phi$ | $5.16 \cdot 10^{-4}$ | $4.28 \cdot 10^{-3}$ |

and  $p_T$ ), background normalization (Tables 1–4),  $Z$  boson production cross section (2.5%) [42], lepton identification and isolation efficiency (1.0%), and trigger efficiency (1.0%). The tau-identification efficiency uncertainty is estimated to be 7% from an independent study done using a tag-and-probe technique [42] including the uncertainty of the trigger efficiency. The lepton identification and isolation efficiencies are stable as a function of the number of additional interactions in the bunch crossing in data and in Monte Carlo simulation. The  $b$ -tagging efficiency has an uncertainty of 10%, and the  $b$ -mistag rate is accurate to 30% [35]. Uncertainties that contribute to mass spectrum shape variations include the tau (3%), muon (1%), and electron (1.5%) energy scales. The effect of the uncertainty on the  $E_T$  scale, mainly due to pile-up effects, is incorporated by varying the mass spectrum shape as described in the next section. The neutral MSSM Higgs production cross sections and the corresponding uncertainties are provided by the LHC Higgs Cross Section Group [44]. The cross sections have been obtained

from the GGH@NNLO [45–49] and HIGLU [50, 51] programs for the gluon-fusion process. For the  $b\bar{b} \rightarrow \Phi$  process, the four-flavour calculation [52, 53] and the five-flavour calculation as implemented in BBH@NNLO [54] have been combined using the Santander scheme [55]. The Rescaling of the corresponding Yukawa couplings to the MSSM calculated with FeynHiggs [56–58] have been applied. The uncertainties for the MSSM signal depends on  $\tan\beta$  and  $M_A$  and can amount up to 25%. The MSTW2008 proton distribution function is used, and the associated uncertainties range from 2-10%. The renormalization and factorization scale uncertainties are 5-25% in the gluon-fusion process and 8-15% in the associated-b process.

## 5 Results

To search for the presence of a Higgs boson signal in the selected events, a binned maximum likelihood fit to the tau-pair invariant-mass spectrum is performed. The fit is performed simultaneously for the four final states with two event categories each. Systematic uncertainties are represented by nuisance parameters in the fitting process. Log-normal priors are assumed for the normalization parameters, and Gaussian priors for mass-spectrum shape uncertainties. The uncertainties that affect the shape of the mass spectrum, mainly those corresponding to the energy scales, are represented by nuisance parameters whose variation results in a continuous perturbation of the spectrum shape.

The signal expectation is determined in each point of the parameter space as follows:

- at each point of  $M_A$  and  $\tan\beta$  the mass, the gluon-fusion and associated- $b$  production cross sections and the branching ratio to  $\tau\tau$  is determined for  $h$ ,  $H$  and  $A$
- for each neutral Higgs boson the expected reconstructed di- $\tau$  mass is obtained using the simulated signal sample with closest mass
- the contributions of all three neutral Higgs boson are added using the corresponding cross sections time branching fraction.

Figure 1 shows the distribution of the tau-pair mass for the four final states in the no B-Tag category, which is more sensitive to the gluon-fusion production mechanism, compared with the background prediction. Figure 2 shows the distribution of the tau-pair mass for the four final states in the B-Tag category, which enhances the sensitivity to the  $b\bar{b} \rightarrow \Phi$  production mechanism.

The invariant mass spectra shows no evidence for the presence of a Higgs boson signal, therefore 95% CL upper bounds on  $\tan\beta$  as a function of the pseudoscalar Higgs boson mass  $M_A$  are set, which are shown in Table 5.

In the fit, signal contributions from  $h$ ,  $H$  and  $A$  production are considered. The relative contributions of gluon fusion and b-associated production are taken for different  $\tan\beta$  values for each mass hypothesis. The  $m_h^{\max}$  scenario is used, and yields conservative expected limits in the  $\tan\beta$  and  $M_A$  plane. In this scenario, the parameters are set to the following values:  $M_{\text{SUSY}} = 1$  TeV;  $X_t = 2M_{\text{SUSY}}$ ;  $\mu = 200$  GeV;  $M_{\tilde{g}} = 800$  GeV;  $M_2 = 200$  GeV; and  $A_b = A_t$ , where  $M_{\text{SUSY}}$  is the common soft-SUSY-breaking squark mass of the third generation;  $X_t = A_t - \mu / \tan\beta$  is the stop mixing parameter;  $A_t$  and  $A_b$  are the stop and sbottom trilinear couplings, respectively;  $\mu$  the Higgsino mass parameter;  $M_{\tilde{g}}$  the gluino mass; and  $M_2$  is the SU(2)-gaugino mass parameter. The value of  $M_1$  is fixed via the unification relation  $M_1 = (5/3)M_2 \sin\theta_W / \cos\theta_W$ .

Figure 3 shows the 95% CL exclusion in the  $\tan\beta$ - $M_A$  parameter space for the MSSM  $m_h^{\max}$  scenario. The exclusion limits from the LEP experiments are also shown.

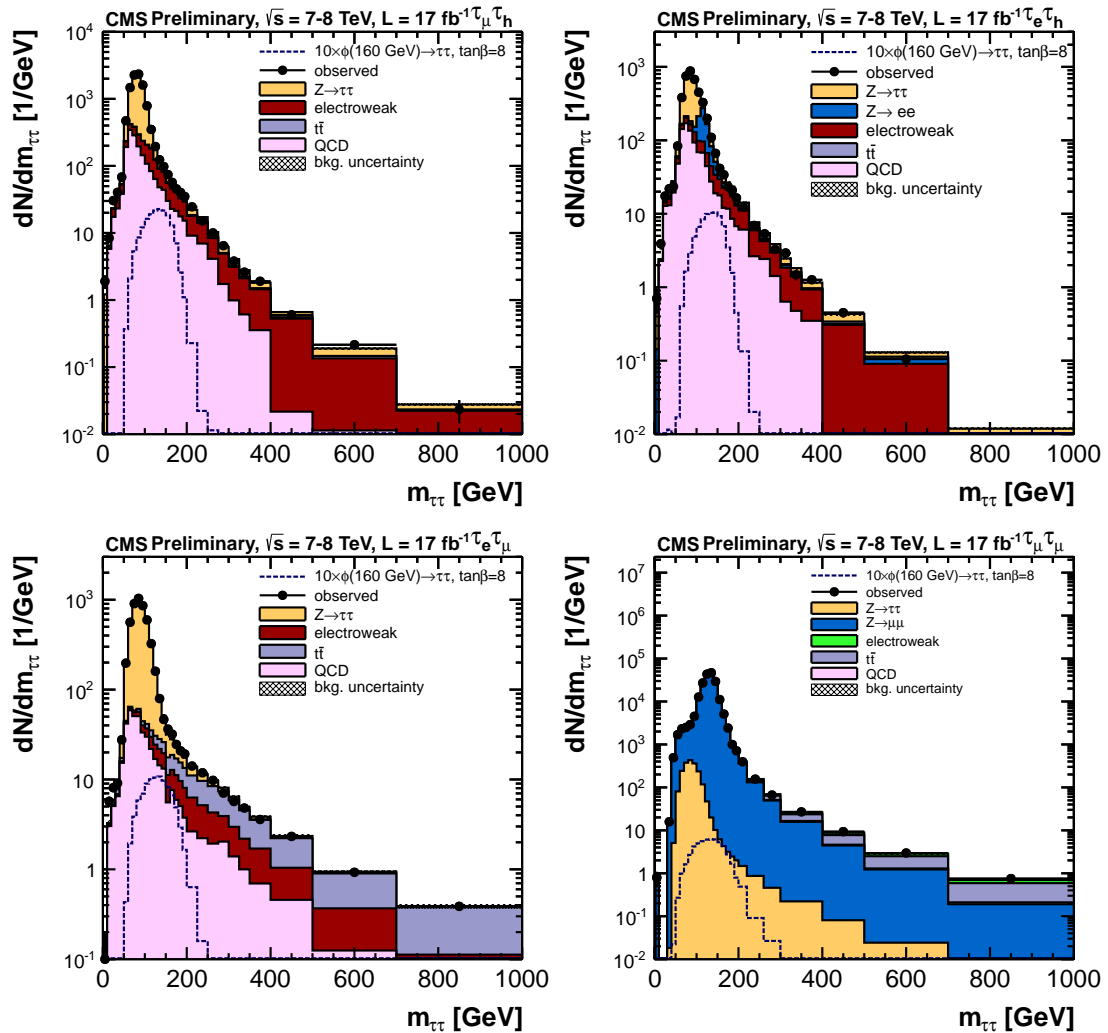


Figure 1: Reconstructed di- $\tau$  mass in the no b-tag category for the  $\mu\tau_h$ ,  $e\tau_h$ ,  $e\mu$  and  $\mu\mu$  channels.

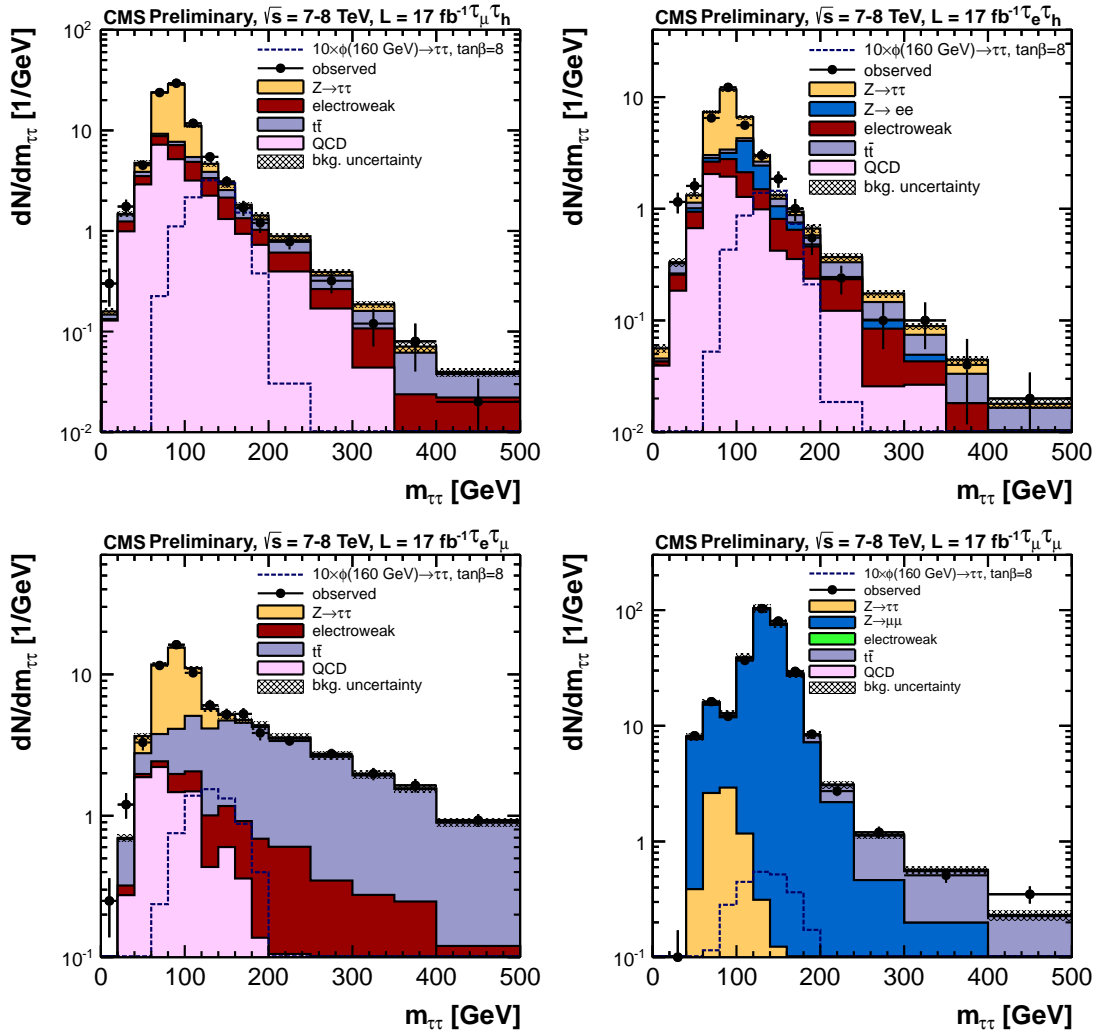


Figure 2: Reconstructed di- $\tau$  mass in the b-tag category for the  $\mu\tau_h$ ,  $e\tau_h$ ,  $e\mu$  and  $\mu\mu$  channels.

Table 5: Expected range and observed 95% CL upper limits for  $\tan \beta$  as a function of  $M_A$ , for the MSSM search.

| MSSM Higgs  | Expected $\tan \beta$ limit |            |        |            |            | Obs. $\tan \beta$ limit |
|-------------|-----------------------------|------------|--------|------------|------------|-------------------------|
| $m_A$ [GeV] | $-2\sigma$                  | $-1\sigma$ | Median | $+1\sigma$ | $+2\sigma$ |                         |
| 90 GeV      | 3.05                        | 3.60       | 7.66   | 8.92       | 10.11      | 4.58                    |
| 130 GeV     | 1.00                        | 4.05       | 4.99   | 5.71       | 6.33       | 4.93                    |
| 140 GeV     | 3.77                        | 4.59       | 5.24   | 5.76       | 6.21       | 5.37                    |
| 200 GeV     | 3.76                        | 4.29       | 7.33   | 8.40       | 9.19       | 3.69                    |
| 250 GeV     | 4.20                        | 8.02       | 9.13   | 10.57      | 12.64      | 5.17                    |
| 300 GeV     | 4.41                        | 10.30      | 12.35  | 14.32      | 16.10      | 7.58                    |
| 350 GeV     | 10.76                       | 13.53      | 15.78  | 18.19      | 20.52      | 10.35                   |
| 400 GeV     | 13.10                       | 16.24      | 18.97  | 21.66      | 24.41      | 13.48                   |
| 450 GeV     | 16.14                       | 19.42      | 22.61  | 25.94      | 29.17      | 17.05                   |
| 500 GeV     | 18.97                       | 22.86      | 26.65  | 30.70      | 34.52      | 20.65                   |
| 600 GeV     | 24.79                       | 30.23      | 35.75  | 41.24      | 46.59      | 29.62                   |
| 700 GeV     | 32.41                       | 39.80      | 47.33  | 55.27      | 62.96      | 39.23                   |
| 800 GeV     | 40.86                       | 50.90      | 61.15  | 73.96      | 98.27      | 48.41                   |

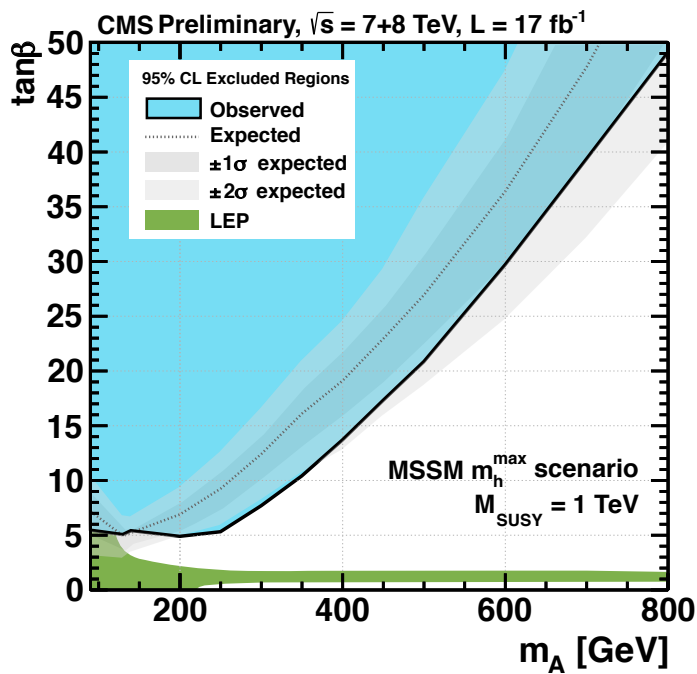


Figure 3: Exclusion at 95% CL in the  $\tan \beta$ - $M_A$  parameter space for the MSSM  $m_h^{\max}$  scenario. The exclusion limits from the LEP experiments are also shown.

## 6 Summary

A search for neutral Higgs bosons decaying to tau pairs has been performed using events recorded by the CMS experiment at the LHC in 2011 and 2012 at a center-of-mass energy of 7 TeV and 8 TeV respectively. The dataset corresponds to an integrated luminosity of  $17 \text{ fb}^{-1}$ , with  $4.9 \text{ fb}^{-1}$  at 7 TeV and  $12.1 \text{ fb}^{-1}$  at 8 TeV. Four different  $\tau\tau$  final states are studied where one or two taus decay leptonically  $e\tau_h, \mu\tau_h, e\mu$  and  $\mu\mu$ . To enhance the sensitivity to neutral Higgs bosons from the minimal supersymmetric extension of the standard model (MSSM), the search includes the case where the Higgs boson is produced in association with a b-quark jet. No excess is observed in the tau-pair invariant-mass spectrum. Exclusion limits in the MSSM parameter space have been obtained for the  $m_h^{\max}$  scenario. This search extends previous results to larger values of  $M_A$  and excluded values of  $\tan\beta$  as low as 4 at  $M_A = 200$  GeV.

## References

- [1] S. L. Glashow, “Partial Symmetries of Weak Interactions”, *Nucl. Phys.* **22** (1961) 579, doi:10.1016/0029-5582(61)90469-2.
- [2] S. Weinberg, “A Model of Leptons”, *Phys. Rev. Lett.* **19** (1967) 1264, doi:10.1103/PhysRevLett.19.1264.
- [3] A. Salam, “Weak and electromagnetic interactions”, in *Elementary particle physics: relativistic groups and analyticity*, N. Svartholm, ed., p. 367. Almqvist & Wiksell, Stockholm, 1968. Proceedings of the eighth Nobel symposium.
- [4] F. Englert and R. Brout, “Broken symmetry and the mass of gauge vector mesons”, *Phys. Rev. Lett.* **13** (1964) 321, doi:10.1103/PhysRevLett.13.321.
- [5] P. W. Higgs, “Broken symmetries, massless particles and gauge fields”, *Phys. Lett.* **12** (1964) 132, doi:10.1016/0031-9163(64)91136-9.
- [6] P. W. Higgs, “Broken symmetries and the masses of gauge bosons”, *Phys. Rev. Lett.* **13** (1964) 508, doi:10.1103/PhysRevLett.13.508.
- [7] G. S. Guralnik, C. R. Hagen, and T. W. B. Kibble, “Global conservation laws and massless particles”, *Phys. Rev. Lett.* **13** (1964) 585, doi:10.1103/PhysRevLett.13.585.
- [8] P. W. Higgs, “Spontaneous symmetry breakdown without massless bosons”, *Phys. Rev.* **145** (1966) 1156, doi:10.1103/PhysRev.145.1156.
- [9] T. W. B. Kibble, “Symmetry breaking in non-Abelian gauge theories”, *Phys. Rev.* **155** (1967) 1554, doi:10.1103/PhysRev.155.1554.
- [10] Y. Golfand and E. Likhtman, “Extension of the Algebra of Poincare Group Generators and Violation of p Invariance”, *JETP Lett.* **13** (1971) 323–326.
- [11] J. Wess and B. Zumino, “Supergauge Transformations in Four-Dimensions”, *Nucl. Phys.* **B70** (1974) 39–50, doi:10.1016/0550-3213(74)90355-1.
- [12] P. Fayet, “Supergauge invariant extension of the Higgs mechanism and a model for the electron and its neutrino”, *Nucl. Phys. B* **90** (1975) 104, doi:10.1016/0550-3213(75)90636-7.

- [13] P. Fayet, "Spontaneously broken supersymmetric theories of weak, electromagnetic and strong interactions", *Phys. Lett. B* **69** (1977) 489, doi:10.1016/0370-2693(77)90852-8.
- [14] CMS Collaboration, "The CMS experiment at the CERN LHC", *JINST* **3** (2008) S08004, doi:10.1088/1748-0221/3/08/S08004.
- [15] CMS Collaboration, "Search for neutral MSSM Higgs bosons decaying to tau pairs in  $pp$  collisions at  $\sqrt{s} = 7$  TeV", *Phys. Rev. Lett.* **106** (2011) 231801, doi:10.1103/PhysRevLett.106.231801.
- [16] ATLAS Collaboration, "Search for neutral MSSM Higgs bosons decaying to  $\tau^+\tau^-$  pairs in proton-proton collisions at  $\sqrt{s} = 7$  TeV with the ATLAS detector", *Phys. Lett. B* **705** (2011) 174, doi:10.1016/j.physletb.2011.10.001.
- [17] CDF and D0 Collaborations, "Combined CDF and D0 Upper Limits on MSSM Higgs Boson Production in Tau-Tau Final States with up to  $2.2 \text{ fb}^{-1}$ ", (2010). arXiv:hep-ex/1003.3363.
- [18] D0 Collaboration, "Search for Higgs bosons decaying to  $\tau^+\tau^-$  pairs in  $p\bar{p}$  collisions at  $\sqrt{s} = 1.96$  TeV", *Phys. Lett. B* **707** (2012) 323, doi:10.1016/j.physletb.2011.12.050.
- [19] CDF Collaboration, "Search for Higgs Bosons Predicted in Two-Higgs-Doublet Models via Decays to Tau Lepton Pairs in 1.96 TeV  $p\bar{p}$  Collisions", *Phys. Rev. Lett.* **103** (2009) 201801, doi:10.1103/PhysRevLett.103.201801.
- [20] LEP Collaborations ALEPH, DELPHI, L3 and OPAL Collaborations and the LEP Working Group for Higgs Boson Searches Collaboration, "Search for neutral MSSM Higgs bosons at LEP", *Eur. Phys. J. C* **47** (2006) 547, doi:10.1140/epjc/s2006-02569-7.
- [21] M. S. Carena et al., "MSSM Higgs boson searches at the Tevatron and the LHC: Impact of different benchmark scenarios", *Eur. Phys. J. C* **45** (2006) 797, doi:10.1140/epjc/s2005-02470-y.
- [22] M. S. Carena et al., "Suggestions for benchmark scenarios for MSSM Higgs boson searches at hadron colliders", *Eur. Phys. J. C* **26** (2003) 601, doi:10.1140/epjc/s2002-01084-3.
- [23] CMS Collaboration Collaboration, "Observation of a new boson at a mass of 125 GeV with the CMS experiment at the LHC", *Phys.Lett. B* **716** (2012) 30–61, doi:10.1016/j.physletb.2012.08.021, arXiv:1207.7235.
- [24] ATLAS Collaboration Collaboration, "Observation of a new particle in the search for the Standard Model Higgs boson with the ATLAS detector at the LHC", *Phys.Lett. B* **716** (2012) 1–29, doi:10.1016/j.physletb.2012.08.020, arXiv:1207.7214.
- [25] S. Heinemeyer, O. Stal, and G. Weiglein, "Interpreting the LHC Higgs Search Results in the MSSM", *Phys.Lett. B* **710** (2012) 201–206, doi:10.1016/j.physletb.2012.02.084, arXiv:1112.3026.
- [26] CMS Collaboration, "Electron Reconstruction and Identification at  $\sqrt{s} = 7$  TeV", CMS Physics Analysis Summary CMS-PAS-EGM-10-004, (2010).
- [27] CMS Collaboration, "Performance of muon identification in  $pp$  collisions at  $\sqrt{s} = 7$  TeV", CMS Physics Analysis Summary CMS-PAS-MUO-10-002, (2010).

[28] CMS Collaboration, “Measurement of Inclusive Z Cross Section via Decays to Tau Pairs in pp Collisions at  $\sqrt{s}=7$  TeV”, *JHEP* **8** (2011) 117, doi:10.1007/JHEP08(2011)117.

[29] CMS Collaboration, “Particle-Flow Event Reconstruction in CMS and Performance for Jets, Taus, and  $E_T^{\text{miss}}$ ”, CMS Physics Analysis Summary CMS-PAS-PFT-09-001, (2009).

[30] CMS Collaboration, “Commissioning of the Particle-Flow Reconstruction in Minimum-Bias and Jet Events from pp Collisions at 7 TeV”, CMS Physics Analysis Summary CMS-PAS-PFT-10-002, (2010).

[31] CMS Collaboration, “Commissioning of the particle-flow event reconstruction with leptons from  $J/\Psi$  and W decays at 7 TeV”, CMS Physics Analysis Summary CMS-PAS-PFT-10-003, (2010).

[32] M. Cacciari, G. P. Salam, and G. Soyez, “FastJet user manual”, arXiv:hep-ph/1111.6097v1.

[33] M. Cacciari and G. P. Salam, “Dispelling the  $N^3$  myth for the  $k_t$  jet-finder”, *Phys. Lett. B* **641** (2006) 57, doi:10.1016/j.physletb.2006.08.037, arXiv:hep-ph/0512210.

[34] CMS Collaboration, “Performance of tau-lepton reconstruction and identification in CMS”, *JINST* **7** (2012) P01001, doi:10.1088/1748-0221/7/01/P01001.

[35] CMS Collaboration, “b-Jet Identification in the CMS Experiment”, CMS Physics Analysis Summary CMS-PAS-BTV-11-004, (2012).

[36] M. Cacciari and G. P. Salam, “Pileup subtraction using jet areas”, *Phys. Lett. B* **659** (2008) 119, doi:10.1016/j.physletb.2007.09.077, arXiv:hep-ph/0707.1378.

[37] CMS Collaboration, “Determination of Jet Energy Calibration and Transverse Momentum Resolution in CMS”, *JINST* **6** (2011) 11002, doi:10.1088/1748-0221/6/11/P11002.

[38] J. Alwall et al., “MadGraph/MadEvent v4: the new web generation”, *JHEP* **09** (2007) 028, doi:10.1088/1126-6708/2007/09/028, arXiv:hep-ph/0706.2334.

[39] T. Sjöstrand, S. Mrenna, and P. Skands, “PYTHIA 6.4 physics and manual”, *JHEP* **05** (2006) 026, doi:10.1088/1126-6708/2006/05/026.

[40] S. Frixione, P. Nason, C. Oleari, “Matching NLO QCD computations with parton shower simulations: the POWHEG method”, *JHEP* **11** (2007) 070, doi:10.1088/1126-6708/2007/11/070.

[41] Z. Wąs, “TAUOLA the library for tau lepton decay, and KKMC/KORALB/KORALZ...status report”, *Nucl. Phys. B, Proc. Suppl.* **98** (2001) 96, doi:10.1016/S0920-5632(01)01200-2.

[42] CMS Collaboration, “Measurement of Inclusive W and Z Cross Sections in  $pp$  Collisions  $\sqrt{s}=7$  TeV”, *JHEP* **1110** (2011) 132, doi:10.1007/JHEP01(2011)080.

[43] CMS Collaboration, “Measurement of CMS Luminosity”, CMS Physics Analysis Summary CMS-PAS-EWK-10-004, (2010).

[44] LHC Higgs Cross Section Working Group, “Handbook of LHC Higgs Cross Sections: 1. Inclusive Observables”, CERN Report CERN-2011-002, (2011).

[45] R. V. Harlander and W. B. Kilgore, “Next-to-next-to-leading order Higgs production at hadron colliders”, *Phys. Rev. Lett.* **88** (2002) 201801, doi:10.1103/PhysRevLett.88.201801, arXiv:hep-ph/0201206.

[46] C. Anastasiou and M. Charalampou, “Higgs boson production at hadron colliders in NNLO QCD”, *Nucl. Phys. B* **646** (2002) 220, doi:10.1016/S0550-3213(02)00837-4, arXiv:hep-ph/0207004.

[47] V. Ravindran, J. Smith, and W. L. van Neerven, “NNLO corrections to the total cross section for Higgs boson production in hadron hadron collisions”, *Nucl. Phys. B* **665** (2003) 325, doi:10.1016/S0550-3213(03)00457-7, arXiv:hep-ph/0302135.

[48] R. V. Harlander and W. B. Kilgore, “Production of a pseudo-scalar Higgs boson at hadron colliders at next-to-next-to leading order”, *JHEP* **10** (2002) 017, doi:10.1088/1126-6708/2002/10/017.

[49] C. Anastasiou and K. Melnikov, “Pseudoscalar Higgs boson production at hadron colliders in NNLO QCD”, *Phys. Rev. D* **67** (2003) 037501, doi:10.1103/PhysRevD.67.037501, arXiv:hep-ph/0208115.

[50] M. Spira, A. Djouadi, D. Graudenz et al., “Higgs boson production at the LHC”, *Nucl. Phys. B* **453** (1995) 17, doi:10.1016/0550-3213(95)00379-7.

[51] M. Spira, “HIGLU: A Program for the Calculation of the Total Higgs Production Cross Section at Hadron Colliders via Gluon Fusion including QCD Corrections”, arXiv:hep-ph/9510347.

[52] S. Dittmaier, M. Kramer, and M. Spira, “Higgs radiation off bottom quarks at the Tevatron and the LHC”, *Phys. Rev. D* **70** (2004) 074010, doi:10.1103/PhysRevD.70.074010.

[53] S. Dawson, C. Jackson, L. Reina et al., “Exclusive Higgs boson production with bottom quarks at hadron colliders”, *Phys. Rev. D* **69** (2004) 074027, doi:10.1103/PhysRevD.69.074027, arXiv:hep-ph/0311067.

[54] R. V. Harlander and W. B. Kilgore, “Higgs boson production in bottom quark fusion at next-to-next-to-leading order”, *Phys. Rev. D* **68** (2003) 013001, doi:10.1103/PhysRevD.68.013001.

[55] R. Harlander, M. Kramer, and M. Schumacher, “Bottom-quark associated Higgs-boson production: reconciling the four- and five-flavour scheme approach”, arXiv:hep-ph/1112.3478.

[56] S. Heinemeyer, W. Hollik, and G. Weiglein, “FeynHiggs: a program for the calculation of the masses of the neutral CP-even Higgs bosons in the MSSM”, *Comput. Phys. Commun.* **124** (2000) 76–89, doi:10.1016/S0010-4655(99)00364-1.

[57] S. Heinemeyer, W. Hollik, and G. Weiglein, “The Masses of the neutral CP-even Higgs bosons in the MSSM: Accurate analysis at the two loop level”, *Eur. Phys. J. C* **9** (1999) 343, doi:10.1007/s100529900006.

[58] G. Degrassi et al., “Towards high-precision predictions for the MSSM Higgs sector”, *Eur. Phys. J. C* **28** (2003) 133, doi:10.1140/epjc/s2003-01152-2.